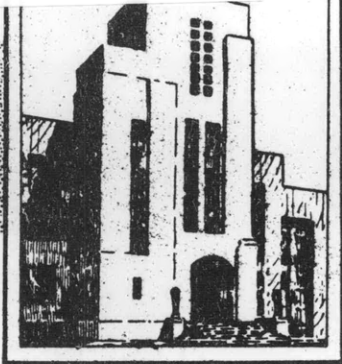


V393
.R46



NAVY DEPARTMENT
DAVID TAYLOR MODEL BASIN

HYDROMECHANICS

○

AERODYNAMICS

○

STRUCTURAL
MECHANICS

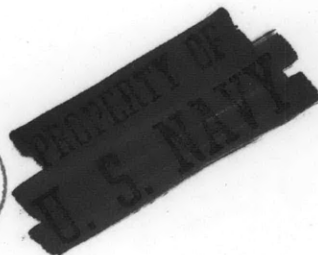
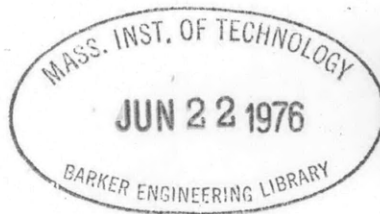
○

APPLIED
MATHEMATICS

THE STRESSES AROUND A RECTANGULAR OPENING WITH
ROUNDED CORNERS IN A BEAM SUBJECTED TO BENDING
WITH SHEAR

by

S.R. Heller, Jr., J.S. Brock and R. Bart



STRUCTURAL MECHANICS LABORATORY
RESEARCH AND DEVELOPMENT REPORT

March 1959

Report 1311

DEPARTMENT OF THE NAVY
DAVID TAYLOR MODEL BASIN
WASHINGTON 7. D.C.

IN REPLY REFER TO
S29/12
A9/1
(710:MCC:1kg)
Ser 7-72
7 Apr 1959

From: Commanding Officer and Director
To: Chief, Bureau of Ships (312) (in duplicate)

Subj: NS731-037, Stresses around openings; forwarding of report on

Encl: (1) TMB Report 1311 entitled, "The Stresses around a
Rectangular Opening with Rounded Corners in a Beam
Subjected to Bending with Shear" 12 copies

1. As part of Project NS731-037 the David Taylor Model Basin has been studying stress distributions around different shapes of openings. Reports have been published on analytical studies of the stresses around circular and square openings and around rectangular openings with rounded corners in a uniformly loaded plate. In enclosure (1) a solution is presented for the stresses around a rectangular opening with rounded corners in a beam subjected to bending with shear. The numerical cases presented are sufficient to cover most openings found in engineering structures.

2. The investigation is being continued to develop a solution for reinforced openings.


E. E. JOHNSON
By direction

Copy to:
BUSHIPS (106)
(420)
(421)
(440)
(442)
(443)

CHONR, Mech Br (438) (with 2 copies of encl (1))
CO, USN Admin Unit, MIT (with 1 copy of encl (1))
OinC, Webb Inst (with 1 copy of encl (1)) ←

THE STRESSES AROUND A RECTANGULAR OPENING WITH ROUNDED
• CORNERS IN A BEAM SUBJECTED TO BENDING WITH SHEAR

By

S. R. Heller, Jr., J.S. Brock, and R. Bart

March 1959

Report 1311

NS731-037

NOTATION

A, B, C, D, E	Real coefficients of mapping function
A_f	Gross area of flanges, $2bt_f$
A_c	Total area of beam
A_w	Gross area of web, $2ht_w$
b	Flange width
e	Eccentricity of center of opening
h	Half-height of beam
I	Moment of inertia of beam
J_o	Stretch ratio at edge of opening
K	Aspect ratio of opening, $2y_o/w$
L	Distance of applied load from center of opening
P	Applied load
r	Corner radius
t_f	Flange thickness
t_w	Web thickness
w	Width of opening
y_o	Half-height of opening, $A - B + C - D + E$
Z	$x + iy$
(x, y)	Cartesian coordinates
(α, β)	Orthogonal curvilinear coordinates

Γ	Shear parameter, a measure of maximum shear stress in web, $\left \frac{\tau_{\max}}{\tau} \right = \frac{3}{2(1 - t_f/h)}$
	$-\frac{h^2 A_w}{2I} \cdot \frac{A_f/A_t}{1 - A_f/A_t}$
ζ	$e^{\alpha + i\beta}$
ρ	Radius ratio, r/w
σ	Nominal bending stress at the extreme fibers at the location of the opening if there were no opening, PLh/I
σ_x, σ_y	Normal stresses; σ_x is normal to the surface; $x = \text{constant}$, etc.
$\sigma_\alpha, \sigma_\beta$	
σ_t	Tangential stress at boundary of opening
τ	Average shear stress at the location of the opening if there were no opening, P/A_w
$\tau_{xy}, \tau_{\alpha\beta}$	Shear stresses

ABSTRACT

A solution for the stresses around a rectangular opening with rounded corners in the web of a beam subjected to bending with shear is presented. The aspect ratio (height to width) and the radius of curvature of the corners are general. The complex-variable method of Muskhelishvili is used in conjunction with a conformal mapping technique to obtain the solution. Curves showing the tangential stress around the boundary of a typical family of rectangles are presented. In addition, curves are given which show the maximum values of the boundary stress as a function of both aspect ratio and corner radius. The numerical cases are sufficient to cover most openings found in engineering structures. The effect of small eccentricity is given in the Appendix.

INTRODUCTION

In the construction of ships, aircraft, and buildings it is frequently necessary, because of space limitations, to pierce the webs of beams for the passage of pipes, electric cables, and ventilation ducts. Moreover, arrangement considerations often make it desirable to group many similar services into the same area with the result that the penetrations are rectangular in shape. Furthermore, for ships—and aircraft carriers in particular, it is necessary to provide rather large access openings in the sides which are essentially

the webs of box girders. Thus the need for knowledge of elastic behavior in the vicinity of these openings is demonstrated.

The simpler geometries have been studied, and the results are readily available, (1)* through (5). The general case of a rectangle with rounded corners which, with suitable simplification, degenerates into the simpler geometries is studied here. The solution which follows is based on the usual assumptions of plane elasticity: homogeneous, isotropic material within the elastic limit, uniform stress across the thickness of the web with no stress normal to the plane of the web, an opening "small" relative to the web (height of opening < 0.25 height of web; edge of opening remote from applied loads), and "small" displacements. The solution is obtained by the complex-variable method associated with Muskhelishvili (6). Although, for ease, the opening is assumed centered on the origin of the coordinate axes, the solution is very general, for the effect of eccentricity is shown in the Appendix.

DETERMINATION OF STRESS DISTRIBUTION CAUSED BY BENDING WITH SHEAR

Consider the loading shown in Figure 1. This loading is equivalent to the sum of the loadings shown in Figures 2a and 2b. These will be examined separately.

* Numbers in parentheses refer to the Bibliography.

PURE BENDING

For the loading shown in Figure 2a the stresses in the web remote from the opening are:

$$\sigma_x = \frac{PLy}{I}; \sigma_y = 0; \tau_{xy} = 0 \quad [1]$$

Using the same mapping function as in (7):

$$z = A\zeta + \frac{B}{\zeta} + \frac{C}{\zeta^3} + \frac{D}{\zeta^5} + \frac{E}{\zeta^7} \quad [2]$$

and following the procedure outlined in (7), we obtain:

$$J_0^2 \left(\frac{\sigma_t}{\frac{PLy_0}{I}} \right) = \frac{A}{y_0} (\Delta_1 \sin\beta + \Delta_3 \sin 3\beta + \Delta_5 \sin 5\beta + \Delta_7 \sin 7\beta + \Delta_9 \sin 9\beta) \quad [3]$$

where σ_t is the tangential stress at the boundary and

$$\Delta_1 = A^2 - a_2' AB + 3a_2' AC - 6a_4' AC + 10a_4' AD - 30K_3 AD + 42K_3 AE - 56E^2$$

$$\Delta_3 = a_2' A^2 - AB - 2a_4' AB - 18K_3 AC + 5a_2' AD - 40DE + 14a_4' AE$$

$$\Delta_5 = 2a_4' A^2 - 6K_3 AB - 3AC - 24CE + 7a_2' AE$$

$$\Delta_7 = AD - 2BE$$

$$\Delta_9 = AE$$

$$J_0^2 = S_0 + S_2 \cos 2\beta + S_4 \cos 4\beta + S_6 \cos 6\beta + S_8 \cos 8\beta$$

$$S_0 = A^2 + B^2 + 9C^2 + 25D^2 + 49E^2$$

$$S_2 = -2(AB - 3BC - 15CD - 35DE)$$

$$S_4 = -2(3AC - 5BD - 21CE)$$

$$S_6 = -2(5AD - 7BE)$$

$$S_8 = -14AE$$

$$y_0 = A - B + C - D + E$$

$$a'_2 = \frac{2K_7 - 1 - 8K_1 K_5}{1 + 2K_3 - 8K_1^2}$$

$$a'_4 = 2(K_5 - K_1 a'_2)$$

$$K_1 = \frac{E}{A}$$

$$K_3 = \frac{D}{A} + \frac{E}{A} K_1$$

$$K_5 = \frac{C}{A} + \frac{B}{A} K_3 + \frac{3C}{A} K_1$$

$$K_7 = \frac{B}{A} + \frac{B}{A} K_5 + \frac{3C}{A} K_3 + \frac{5D}{A} K_1$$

Equation [3] agrees with (3) for the ovaloid ($D = E = 0$), with (2) for the ellipse ($C = D = E = 0$); and with (1) for the circle ($B = C = D = E = 0$).

PURE SHEAR AT Y-AXIS

For the loading shown in Figure 2b the stresses in the web remote from the opening are:

$$\sigma_x = -\frac{Pxy}{I}; \sigma_y = 0; \tau_{xy} = -\tau\Gamma + \frac{Py^2*}{2I} \quad [4]$$

where

$$\tau = \frac{P}{A_w}$$

$$\Gamma = \frac{3}{2\left(1 - \frac{t_f}{h}\right)} - \frac{A_w h^2}{2I} \cdot \frac{A_f/A_t}{1 - A_f/A_t}$$

Using the same mapping function and procedure as in (7), we obtain:

$$J_o^2 \sigma_t = -\frac{PA^2}{2I} \left(\Delta_2 \sin 2\beta + \Delta_4 \sin 4\beta + \Delta_6 \sin 6\beta + \Delta_8 \sin 8\beta + \Delta_{10} \sin 10\beta \right) \quad [5]$$

where

$$\Delta_2 = A^2 + a_1'' A^2 - 3a_3'' AB + 3a_1'' AC - 15a_5'' AC + 15a_3'' AD - 35K_3 AD + 35a_5'' AE - 63E^2$$

$$\Delta_4 = 3a_3'' A^2 - AB - 5a_5'' AB - 21K_3 AC + 5a_1'' AD - 45DE + 21a_3'' AE$$

$$\Delta_6 = 5a_5'' A^2 - 7K_3 AB - 3AC - 27CE + 7a_1'' AE$$

$$\Delta_8 = 2(AD - BE)$$

$$\Delta_{10} = 2AE$$

* This is based on approximate theory which neglects the three-dimensional effect at the junction of flange and web. It agrees well with the approximate theory that the web of an I-beam takes most of the shearing force and that the shearing stresses are constant across the web thickness. Cf. Reference (8), p. 305.

$$a_1'' = \frac{\frac{K_3(2 - 3K_7)}{1 + 3K_1} + K_9 - 5K_1K_5 - \frac{8I\tau\Gamma}{PA^2}}{1 + K_5 - \frac{3K_3^2}{1 + 3K_1} - 5K_1^2}$$

$$a_3'' = -\frac{1}{1 + 3K_1} \left(K_3 a_1'' + \frac{2 - 3K_7}{3} \right)$$

$$a_5'' = K_5 - K_1 a_1''$$

$$K_9 = 1 + \frac{B}{A}K_7 + \frac{3C}{A}K_5 + \frac{5D}{A}K_3 + \frac{7E}{A}K_1$$

Equation [5] agrees with (5) for the ovaloid ($D = E = 0$); with (2) for the ellipse ($C = D = E = 0$) in a rectangular strip ($\Gamma = 1.5$); and with (4) for the circle ($B = C = D = E = 0$) in a rectangular strip ($\Gamma = 1.5$).

The parameter used in (5), the ratio of nominal shear stress (P/A_w) to nominal bending stress (PLh/I), $\tau/\sigma = I/hLA_w$, is now introduced as is the same reference stress used in Equation [3], the nominal bending stress at the edge of the opening if there were no opening, PLy_o/I . When it is considered that $L \gg A, B, C, D, E$, Equation [5] becomes:

$$J_o^2 \left(\frac{\sigma_t}{PLy_o} \right) \cong \frac{4A^2 \frac{\tau}{\sigma} \frac{h}{y_o} \cdot \Gamma}{1 + K_5 - 3K_3^2 - 5K_1^2} \left[\left(1 + 3\frac{C}{A} + 3\frac{BD}{A^2} + 15\frac{CE}{A^2} - 15\frac{D^2}{A^2} - 35\frac{E^2}{A^2} + 3\frac{B^2E}{A^3} - 15\frac{BDE}{A^3} \right) \sin 2\beta \right. \\ \left. + \left(2\frac{D}{A} + 2\frac{BE}{A^2} - 21\frac{DE}{A^2} - 21\frac{BE^2}{A^3} \right) \sin 4\beta + 2\frac{E}{A} \sin 6\beta \right] \quad [5a]$$

If due regard is taken of the relative magnitudes and the signs of the terms, Equation [5a] may be simplified to:

$$J_o^2 \left(\frac{\sigma_t}{\frac{PLy_o}{I}} \right) \cong \frac{4A^2 \frac{\tau}{\sigma} \cdot \frac{h}{y_o} \Gamma}{1 + K_5} \left[\left(1 + 3K_5 + 6\frac{CE}{A^2} - 15\frac{D^2}{A^2} \right) \sin 2\beta \right. \\ \left. + \left(2K_3 - 21\frac{DE}{A^2} \right) \sin 4\beta + 2K_1 \sin 6\beta \right] \quad [5b]$$

If, however, the reference stress is taken as the average shear stress, P/A_w , then Equation [5b] becomes:

$$J_c^2 \left(\frac{\sigma_t}{\frac{P}{A_w}} \right) \cong \frac{4A^2 \Gamma}{1 + K_5} \left[\left(1 + 3K_5 + 6\frac{CE}{A^2} - 15\frac{D^2}{A^2} \right) \sin 2\beta \right. \\ \left. + \left(2K_3 - 21\frac{DE}{A^2} \right) \sin 4\beta + 2K_1 \sin 6\beta \right] \quad [5c]$$

The effect of the loading shown in Figure 1 is the combination of Equations [3] and [5b]:

$$J_o^2 \left(\frac{\sigma_t}{\frac{PLy_o}{I}} \right) = \frac{A}{y_o} (\Delta_1 \sin \beta + \Delta_3 \sin 3\beta + \Delta_5 \sin 5\beta + \Delta_7 \sin 7\beta + \Delta_9 \sin 9\beta) \\ + \frac{4A^2 \frac{\tau}{\sigma} \cdot \frac{h}{y_o} \Gamma}{1 + K_5} \left[\left(1 + 3K_5 + 6\frac{CE}{A^2} - 15\frac{D^2}{A^2} \right) \sin 2\beta \right. \\ \left. + \left(2K_3 - 21\frac{DE}{A^2} \right) \sin 4\beta + 2K_1 \sin 6\beta \right] \quad [6]$$

Although τ/σ may take any value depending on the proportions of the beam (I , A_w , h , and L), the practical range, based on investigations of typical civil engineering and ship structures, is from 0 to 0.4. For values of $\tau/\sigma > 0.5$, σ is either negligibly small so that the maximum stress at the opening, even with a large stress concentration factor, is quite small compared with the maximum stress elsewhere in the beam, or else L is not appreciably larger than the half-width of the opening. In the latter case the local effect of the load predominates—a condition specifically exempted in this development.

NUMERICAL RESULTS

The values of mapping function coefficients for a wide range of aspect and radius ratios are given in Table 1 of (7). It is also shown therein that the fit of the opening so mapped to the actual opening is excellent. Therefore, those same values are used here for all numerical work.

These values are used in conjunction with Equation [6] to obtain the stress distribution. Specifically, the nondimensional stress representation, $\frac{\sigma_t}{PLy_o/I}$, is then calculated for one quadrant, $0 \leq \beta \leq \pi/2$. A sample plot for one particular rectangular opening ($K = 1/2$, $\rho = 1/16$, $y_o/h = 0.1$) in a rectangular strip ($\Gamma = 1.5$) but for the family of shear-to-bending ratios (τ/σ) is shown in Figure 3.

Also shown is the locus and magnitude of $\left(\frac{\sigma_t}{PLy_o/I}\right)_{\max}$ and its dependence on τ/σ . Similarly, a sample plot for the family of rectangular openings with aspect ratio of 1/2 but for a single size of opening ($y_o/h = 0.1$) in a rectangular strip ($\Gamma = 1.5$) and for only one shear-to-bending ratio ($\tau/\sigma = 0.1$) is shown in Figure 4. Also shown is the locus and magnitude of $\left(\frac{\sigma_t}{PLy_o/I}\right)_{\max}$ and its dependence on radius ratio (ρ). Figure 5 shows the locus of $\left(\frac{\sigma_t}{PLy_o/I}\right)_{\max}$ in relation to actual geometry. The salient feature of Figure 5 is the approach of the point of maximum stress to the actual corner with the increase in shear.

Plots similar to Figures 3 and 4 were made for the series of families of rectangular openings defined by Table 1 of (7) but limited to the single size of opening, $y_o/h = 0.1$, and to the rectangular strip, $\Gamma = 1.5$. These results are summarized in Figures 6, 7, 8, 9, and 10 where $\left(\frac{\sigma_t}{PLy_o/I}\right)_{\max}$ is plotted against ρ in contours of K . It can be seen that for the families investigated, $\left(\frac{\sigma_t}{PLy_o/I}\right)_{\max}$ did, for the lower values of τ/σ , pass through a minimum as ρ increased although the minimum became less pronounced as K decreased.

Finally, the most appropriate ρ for a given K , i.e., the ρ for a given K which gives the minimum $\left(\frac{\sigma_t}{PLy_o/I}\right)_{\max}$, is shown in Figure 11 for various τ/σ . A similar plot is given in Figure 12 in which the ordinate is shifted to τ/σ and the contours to K .

ACKNOWLEDGMENTS

The authors wish to express their sincere appreciation to Mrs. Mildred R. Overby who carefully and meticulously performed the many tedious calculations on which Figures 6 through 10 are based. They also desire to extend their gratitude to the Bureau of Ships, Navy Department, for sponsoring the research embodied in this paper.

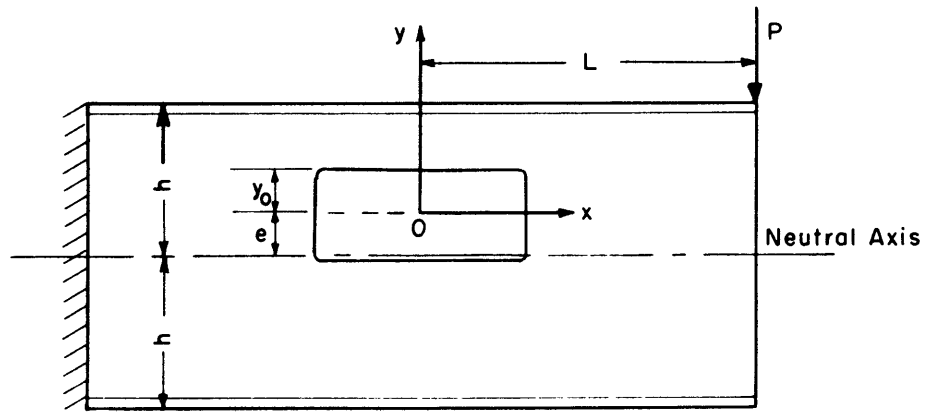


Figure 1 - Geometry of Beam Subjected to Bending with Shear

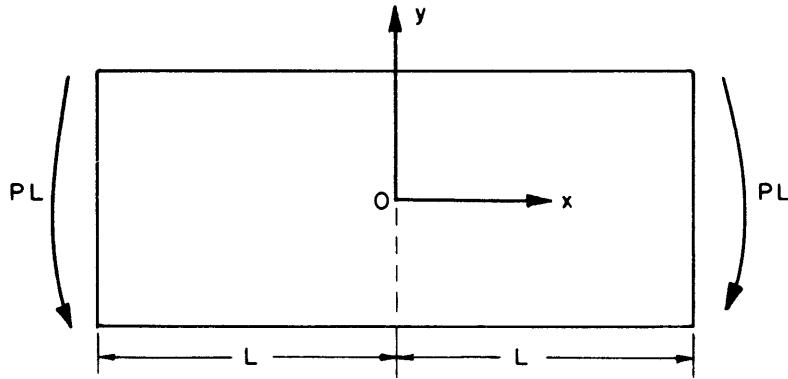


Figure 2a - Pure Bending

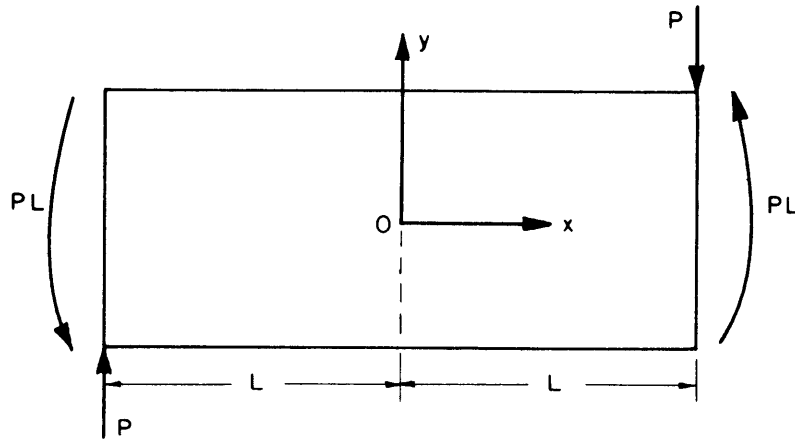


Figure 2b - Pure Shear at Y-Axis

Figure 2 - Schematic Loading of Beam

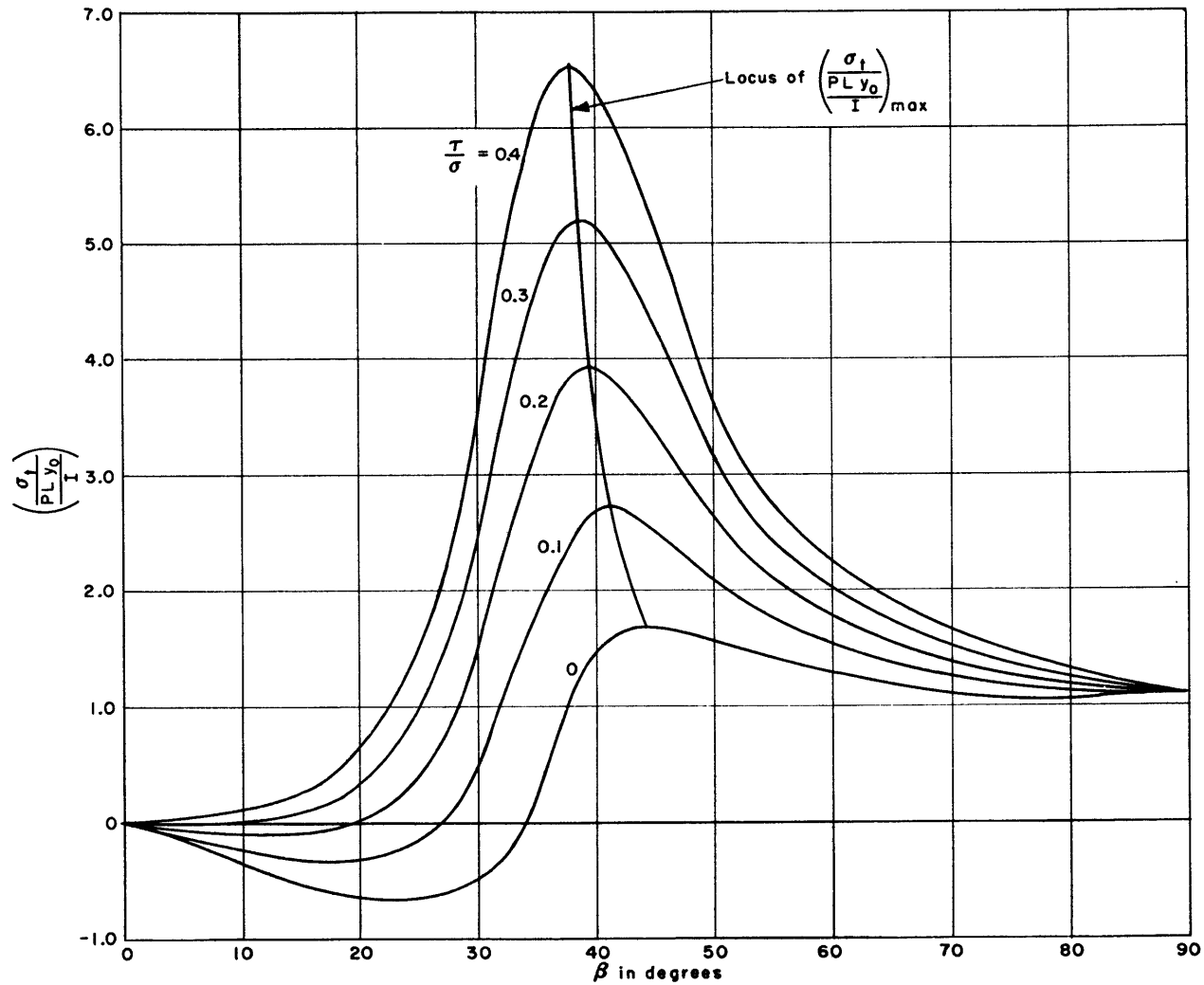


Figure 3 - Typical Tangential Stress Distribution Around the Boundary of One Quadrant in Contours of Shear-to-Bending Ratio, $K = 1/2$, $\rho = 1/16$, $y_0/h = 0.1$, $\Gamma = 1.5$

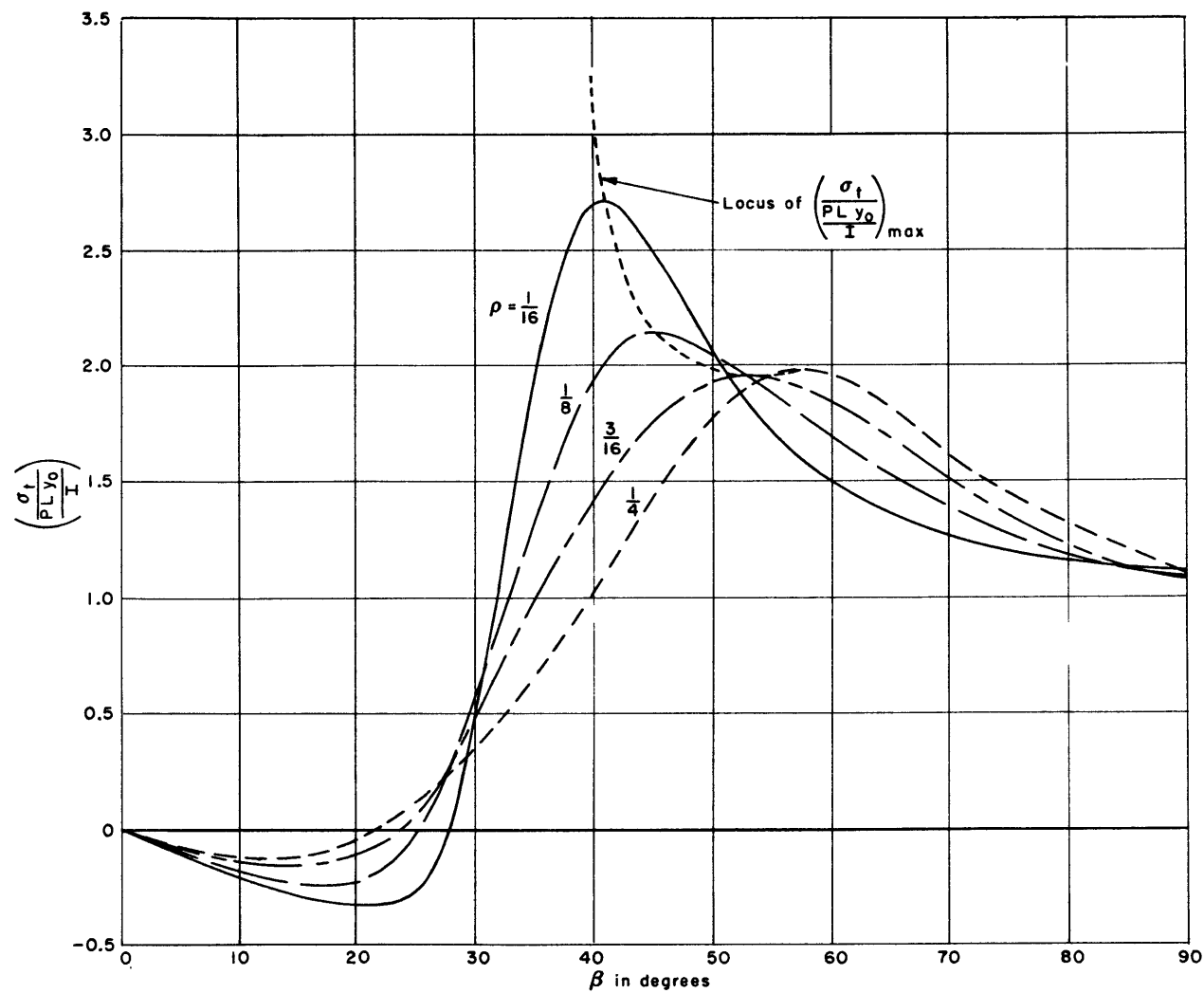


Figure 4 - Typical Tangential Stress Distribution Around the Boundary of One Quadrant in Contours of Radius Ratio, $K = 1/2$, $\tau/\sigma = 0.1$, $y_0/h = 0.1$, $\Gamma = 1.5$

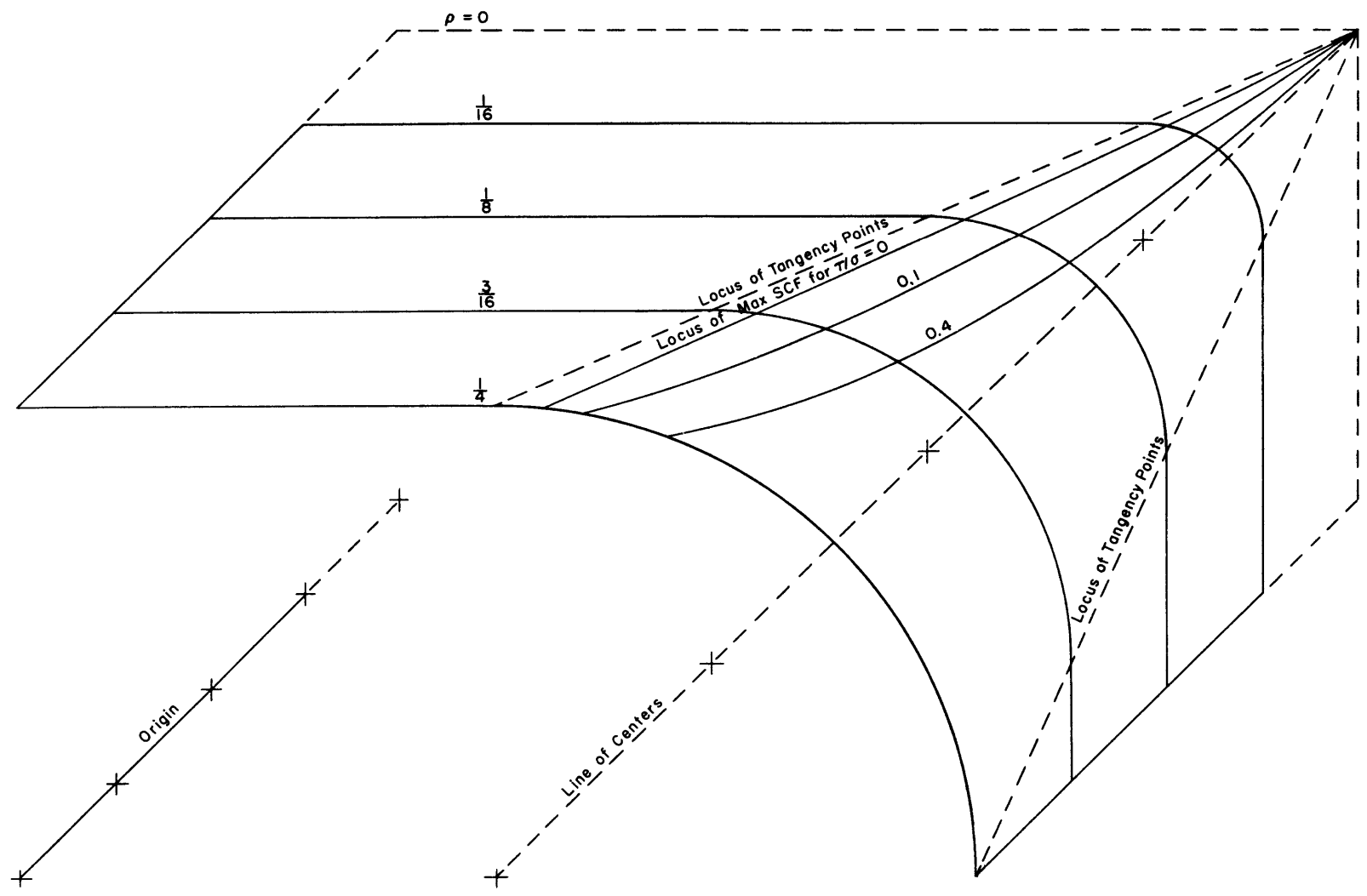


Figure 5 - Location of Maximum Stress, $K = 1/2$, $y_0/h = 0.1$, $\Gamma = 1.5$

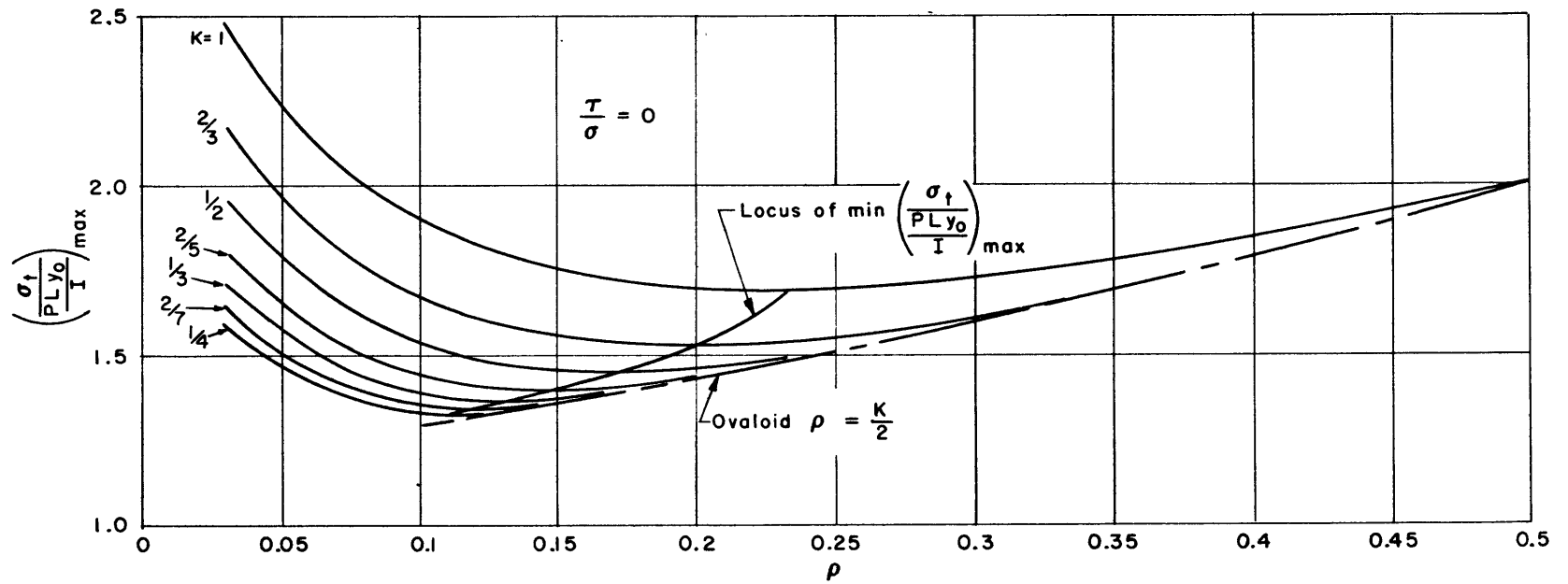


Figure 6 - Maximum Stress Concentration Factor versus Radius Ratio in Contours of Aspect Ratio, $\tau/\sigma = 0$

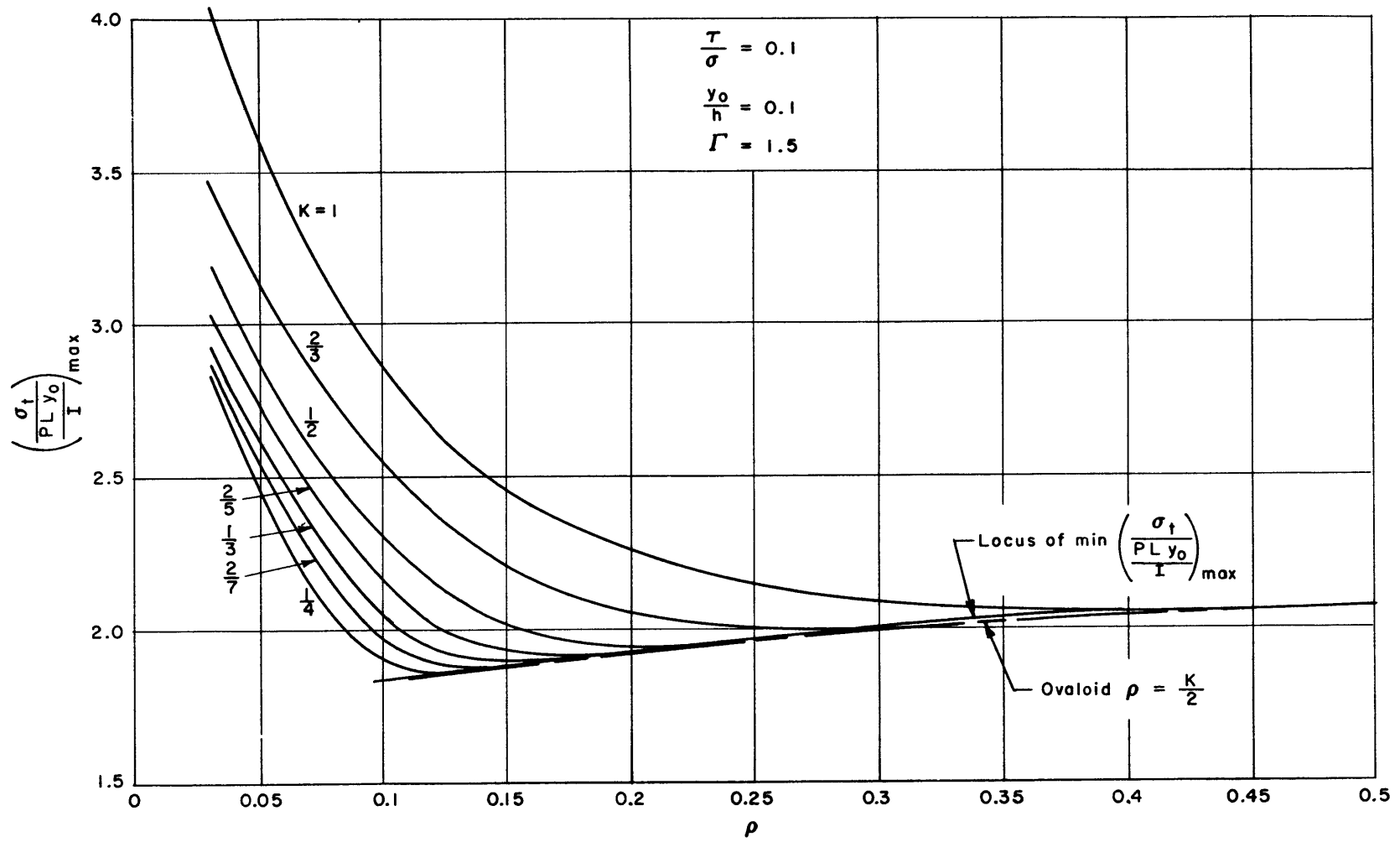


Figure 7 - Maximum Stress Concentration Factor versus Radius Ratio in Contours of Aspect Ratio, $\tau/\sigma=0.1$, $y_0/h = 0.1$, $\Gamma = 1.5$

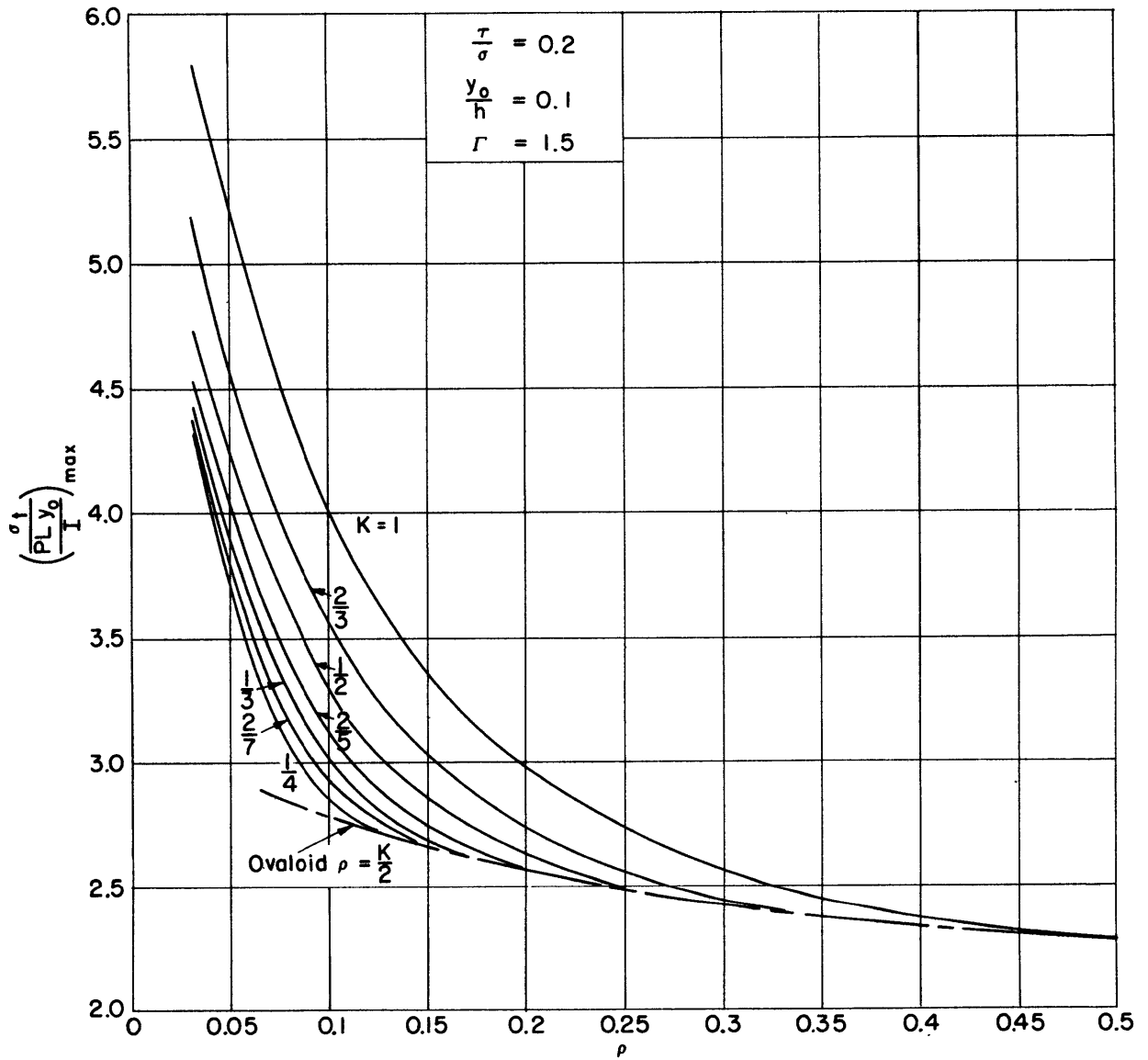


Figure 8 - Maximum Stress Concentration Factor versus Radius Ratio in Contours of Aspect Ratio, $\tau/\sigma = 0.2$, $y_0/h = 0.1$, $\Gamma = 1.5$

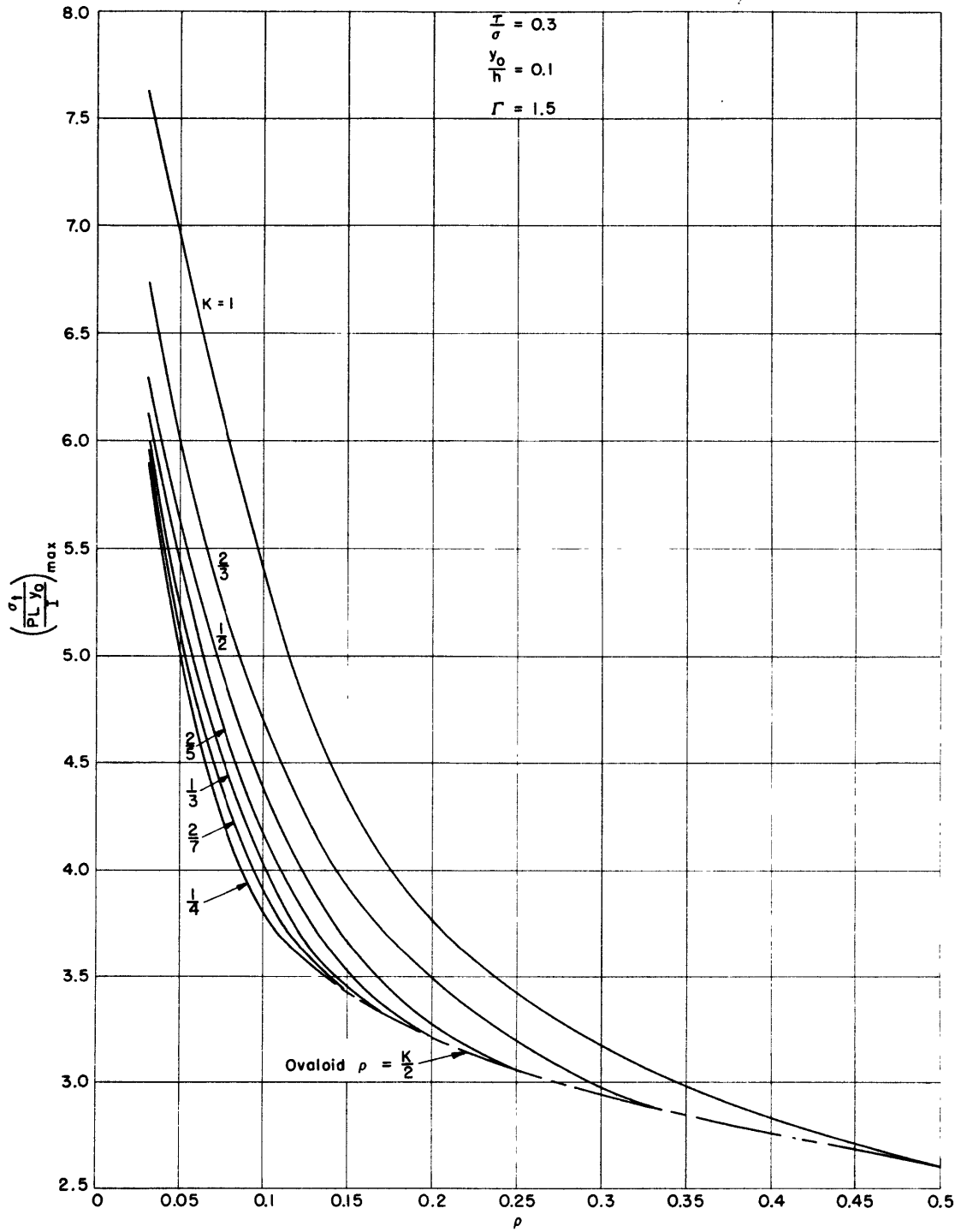


Figure 9 - Maximum Stress Concentration Factor versus Radius Ratio in Contours of Aspect Ratio, $\tau/\sigma = 0.3$, $y_0/h = 0.1$, $\Gamma = 1.5$

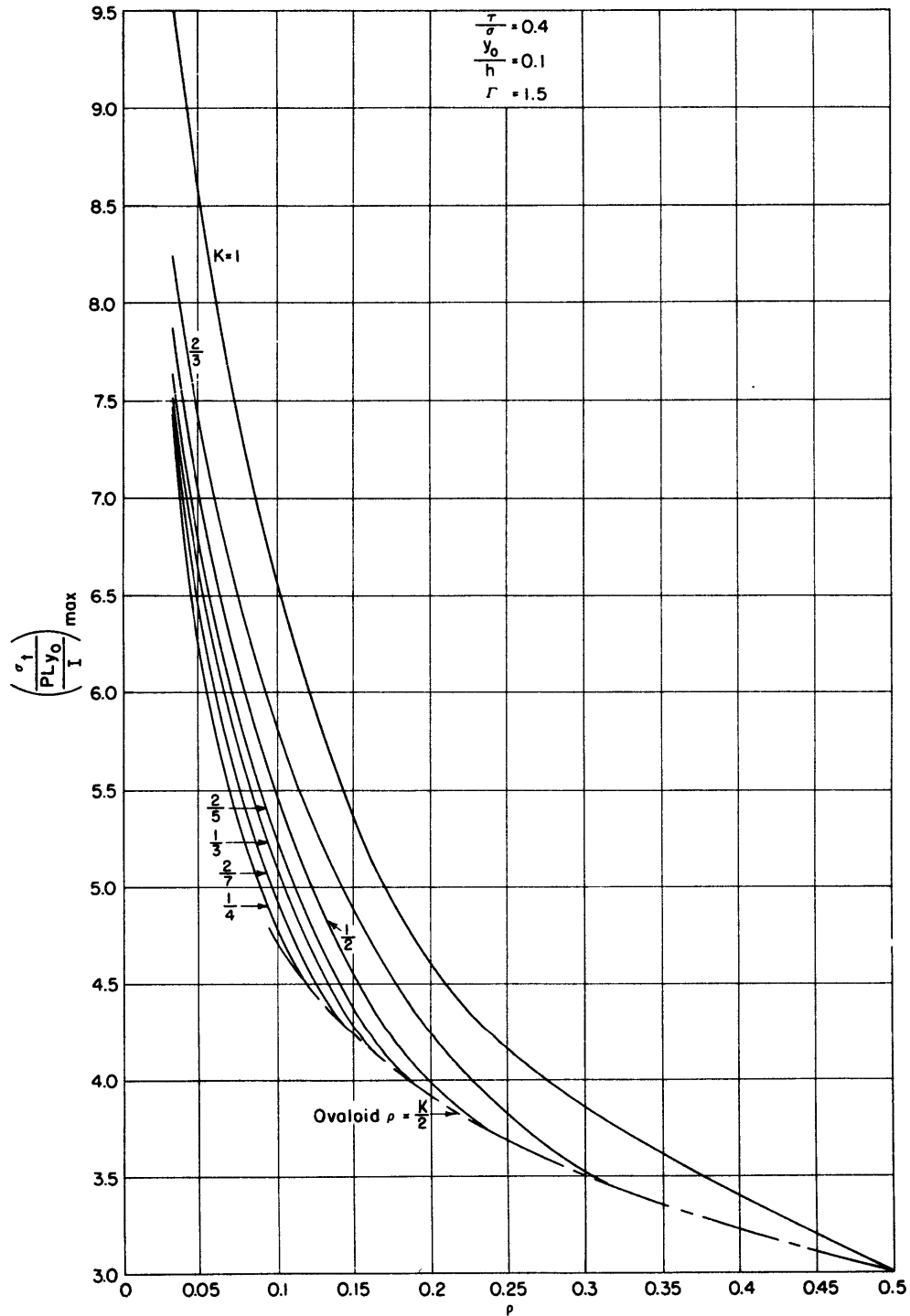


Figure 10 - Maximum Stress Concentration Factor versus Radius Ratio in Contours of Aspect Ratio, $\tau/\sigma = 0.4$, $y_0/h = 0.1$, $\Gamma = 1.5$

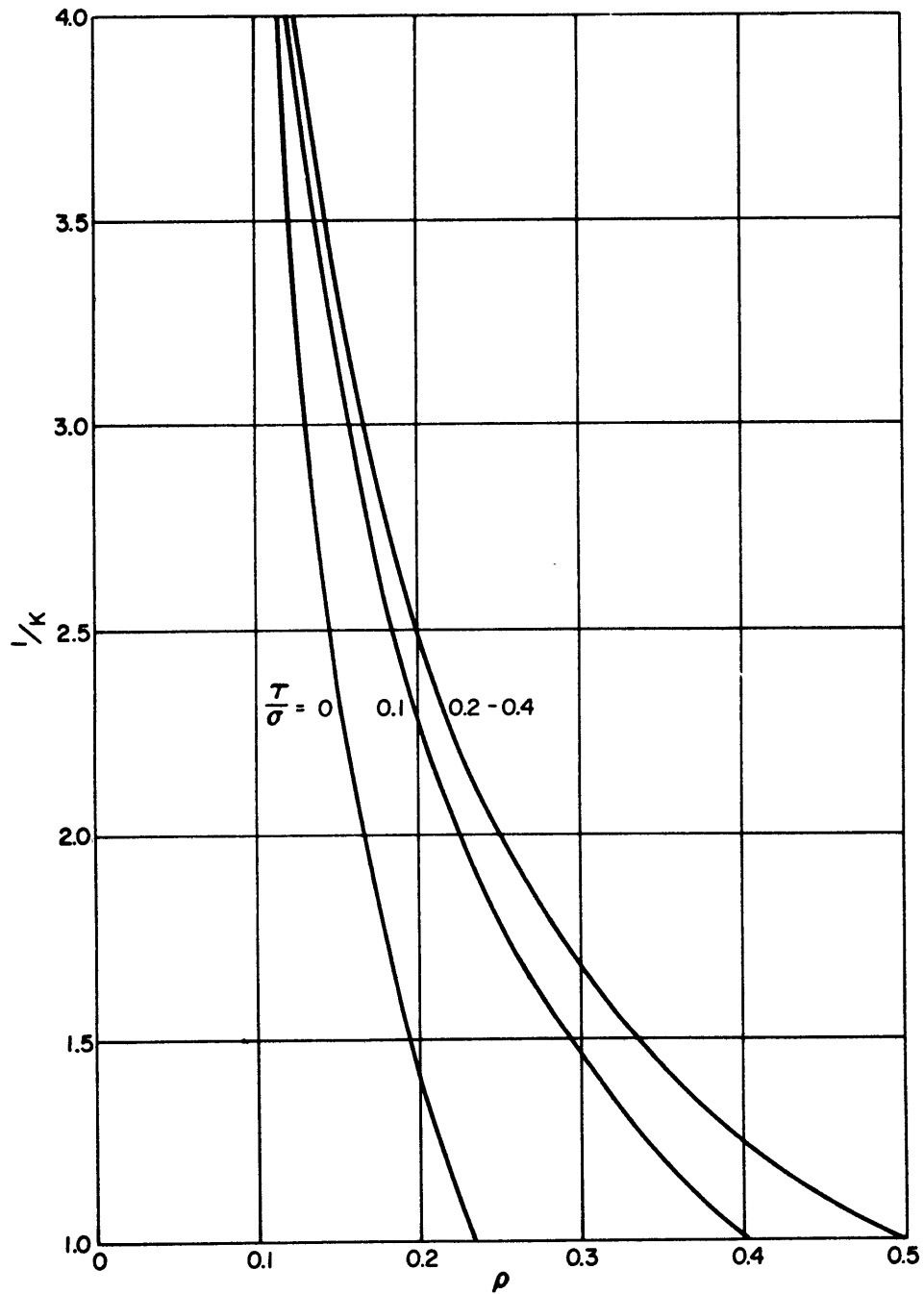


Figure 11 - Relation between Radius and Aspect Ratios for Minimum Stress Concentration Factor in Contours of τ/σ , $y_0/h = 0.1$, $\Gamma = 1.5$

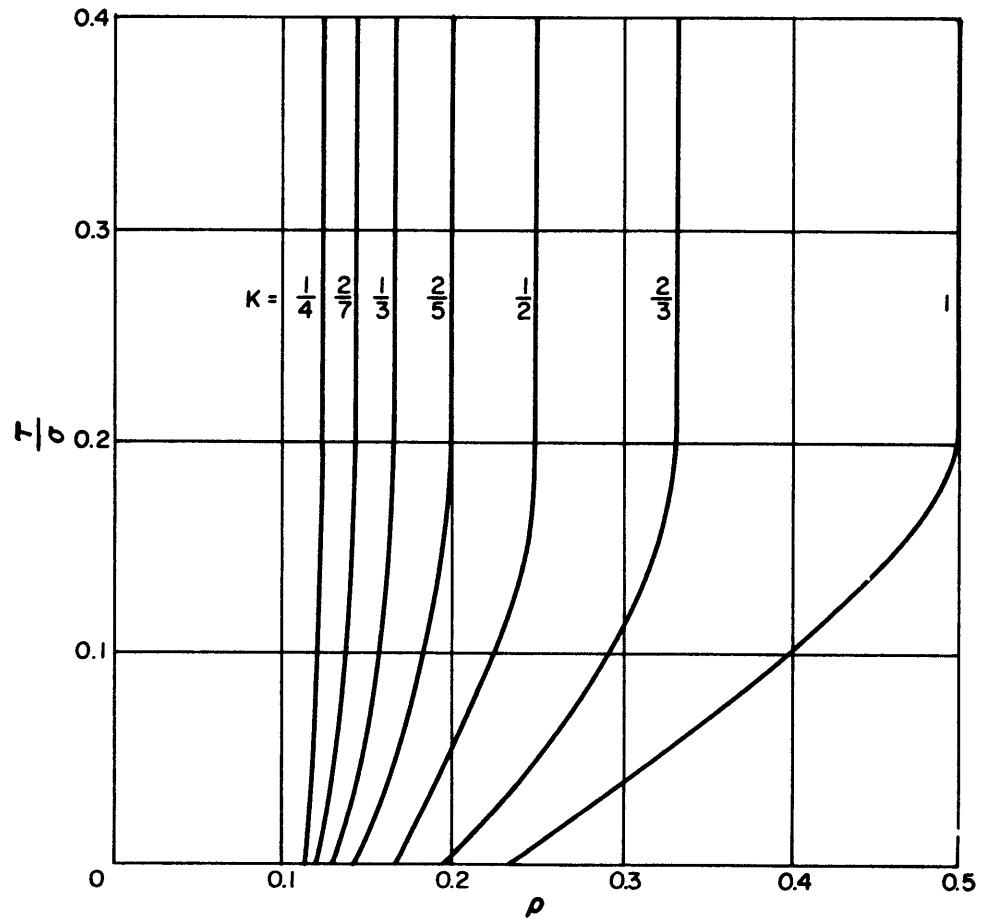


Figure 12 - Relation between Radius and Shear-to-Bending Ratios for Minimum Stress Concentration Factor in Contours of Aspect Ratio, $y_0/h = 0.1$, $\Gamma = 1.5$

APPENDIX

EFFECT OF SMALL ECCENTRICITY

For $x \gg \text{hole}$

$$\sigma_x = \frac{P(L-x)(y+e)}{I}; \sigma_y = 0; \tau_{xy} = -\tau\Gamma + \frac{P(y+e)^2}{2I}.$$

This is equivalent to:

Pure Bending: $\sigma_x = \frac{PLy}{I}; \sigma_y = 0; \tau_{xy} = 0$

+ Shear Effect: $\sigma_x = -\frac{Pxy}{I}; \sigma_y = 0; \tau_{xy} = -\tau\Gamma + \frac{Py^2}{2I}$

+ Uniform Stress (7): $\sigma_x = \frac{PLe}{I}; \sigma_y = 0; \tau_{xy} = 0$

(Eccentricity Effect on Pure Bending)

+ Eccentricity Effect $\sigma_x = -\frac{Pex}{I}; \sigma_y = 0; \tau_{xy} = \frac{Pe(2y+e)}{2I}$

on Shear:

[7]

Now, if Equations [7] are used as boundary conditions along with Equation [2] as before, the results are:

$$J_o^2 \left(\frac{\sigma_t}{\frac{PLy_o}{I}} \right) = -\frac{A}{y_o} \cdot \frac{e}{L} \left[\Delta'_1 \cos\beta + \Delta'_3 \cos 3\beta + \Delta'_5 \cos 5\beta + \Delta'_7 \cos 7\beta + \Delta'_9 \cos 9\beta \right. \\ \left. + 2e \left(N'_2 \sin 2\beta + N'_4 \sin 4\beta + N'_6 \sin 6\beta \right) \right]$$

where $\Delta'_1 = A^2 - a'_2 AB - 3a'_2 AC - 12a'_4 AC - 20a'_4 AD - 30K_3 AD - 42K_3 AE - 56E^2$

$$\Delta'_3 = a'_2 A^2 - AB - 4a'_4 AB - 18K_3 AC - 5a'_2 AD - 40DE - 28a'_4 AE$$

$$\Delta'_5 = 4a'_4 A^2 - 6K_3 AB - 3AC - 24CE - 7a'_2 AE$$

$$\Delta'_7 = 6K_3 A^2 - 8BE - 5AD$$

$$\Delta'_9 = AE$$

$$N'_2 = a'_1 A + 3a'_1 C + 3a'_3 B - 15a'_3 D + 15a'_5 C - 35a'_5 E$$

$$N'_4 = 5a'_1 D - 3a'_3 A - 21a'_3 E + 5a'_5 B$$

$$N'_6 = 7a'_1 E - 5a'_5 E$$

$$a'_1 = \frac{1}{1 + K_5 - 5K_1^2 - \frac{3K_3^2}{1 + 3K_1}}$$

$$a'_2 = \frac{2K_7 + 8K_1 K_5 - 3}{1 - 2K_3 - 8K_1^2}$$

$$a'_3 = \frac{K_3}{1 + 3K_1} a'_1$$

$$a'_4 = K_5 + K_1 a'_2$$

$$a'_5 = K_1 a'_1$$

BIBLIOGRAPHY

1. Tuzi, Z., "Effect of a Circular Hole on the Stress Distribution Under Uniform Bending Moment," Scientific Papers of the Institute of Physical and Chemical Research, Tokyo, Vol. 9, pp. 65-89 (20 Aug 1928).
2. Wolf, K., "Beitrage zur ebenen Elastizitäts—theorie," Zeitschrift für technische Physik, Vol. 2, No. 8, p. 209 (1921) and Vol. 3, No. 5, pp. 160-166 (1922).
3. Joseph, J.A. and Brock, J.S., "The Stresses Around a Small Opening in a Beam Subjected to Pure Bending," Journal of Applied Mechanics, Vol. 17, No. 4, pp. 353-358 (Dec 1950).
4. Howland, R.C.J. and Stevenson, A.C., "Biharmonic Analysis in a Perforated Strip," Philosophic Transactions of the Royal Society of London, Series A, Vol. 232, pp. 155-222 (1933).
5. Heller, S.R., Jr., "The Stresses Around a Small Opening in a Beam Subjected to Bending with Shear," Proceedings of the First National Congress of Applied Mechanics, pp. 239-245 (1951).
6. Muskhelishvili, N.I. (Translated by Radak, J.R.M.), "Some Basic Problems of the Mathematical Theory of Elasticity," P. Noordhoff, Ltd., Groningen, Holland (1953).
7. Heller, S.R., Jr., Brock, J.S. and Bart, R., "The Stresses Around a Rectangular Opening with Rounded Corners in a Uniformly Loaded Plate," Proceedings of the Third National Congress of Applied Mechanics, pp. 357-368 (1958).

8. Timoshenko, S., "Theory of Elasticity," McGraw-Hill Book Company, Inc., New York, N.Y., First Edition (1934).

INITIAL DISTRIBUTION

Copies

12 CHBUSHIPS, Library (Code 312)
 5 Tech Library
 1 Tech Asst to Chief (Code 106)
 1 Prelim Des Br (Code 420)
 1 Prelim Des Sec (Code 421)
 1 Hull Des Br (Code 440)
 2 Sci and Res Sec (Code 442)
 1 Structural Sec (Code 443)
2 CHONR, Mech Br (Code 438)
1 CO, USNAVADMINU MIT
1 O in C, PGSCOL, Webb

David Taylor Model Basin. Report 1311.

THE STRESSES AROUND A RECTANGULAR OPENING WITH ROUNDED CORNERS IN A BEAM SUBJECTED TO BENDING WITH SHEAR, by S.R. Heller, J.S. Brock, and R. Bart. March 1959. 27p. diags., graphs, refs. UNCLASSIFIED

A solution for the stresses around a rectangular opening with rounded corners in the web of a beam subjected to bending with shear is presented. The aspect ratio (height to width) and the radius of curvature of the corners are general. The complex-variable method of Muskhelishvili is used in conjunction with a conformal mapping technique to obtain the solution. Curves showing the tangential stress around the boundary of a typical family of rectangles are presented. In addition, curves are given which show the maximum values of the boundary stress as a function of both aspect ratio and corner radius. The numerical cases are sufficient to cover most openings found in engineering structures. The effect of small eccentricity is given in the Appendix.

- I. Beams - Stresses - Mathematical analysis
- I. Heller, Samuel R.
- II. Brock, Joseph S.
- III. Bart, Robert
- IV. NS731-037

David Taylor Model Basin. Report 1311.

THE STRESSES AROUND A RECTANGULAR OPENING WITH ROUNDED CORNERS IN A BEAM SUBJECTED TO BENDING WITH SHEAR, by S.R. Heller, J.S. Brock, and R. Bart. March 1959. 27p. diags., graphs, refs. UNCLASSIFIED

A solution for the stresses around a rectangular opening with rounded corners in the web of a beam subjected to bending with shear is presented. The aspect ratio (height to width) and the radius of curvature of the corners are general. The complex-variable method of Muskhelishvili is used in conjunction with a conformal mapping technique to obtain the solution. Curves showing the tangential stress around the boundary of a typical family of rectangles are presented. In addition, curves are given which show the maximum values of the boundary stress as a function of both aspect ratio and corner radius. The numerical cases are sufficient to cover most openings found in engineering structures. The effect of small eccentricity is given in the Appendix.

- I. Beams - Stresses - Mathematical analysis
- I. Heller, Samuel R.
- II. Brock, Joseph S.
- III. Bart, Robert
- IV. NS731-037

10

11

12